IEEE Photonics Journal
An IEEE Photonics Society Publication

Open Access

Active Terahertz Polarization Converter Using a Liquid Crystal-Embedded Metal Mesh

Volume 11, Number 6, December 2019

Tomoyuki Sasaki
Yuki Nishie
Masaatsu Kambayashi
Moritsugu Sakamoto
Kohei Noda
Hiroyuki Okamoto
Nobuhiro Kawatsuki
Hiroshi Ono

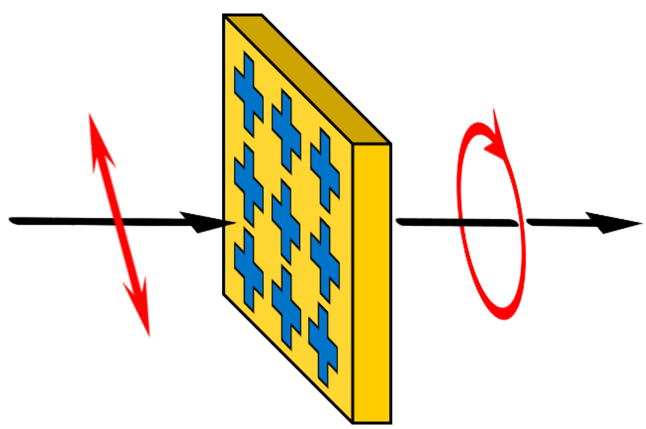

DOI: 10.1109/JPHOT.2019.2950021

IEEE photonics SOCIETY
IEEE

Active Terahertz Polarization Converter Using a Liquid Crystal-Embedded Metal Mesh

Tomoyuki Sasaki,[1] **Yuki Nishie**,[1] **Masaatsu Kambayashi**,[1] **Moritsugu Sakamoto**,[1] **Kohei Noda**,[1] **Hiroyuki Okamoto**,[2] **Nobuhiro Kawatsuki**,[3] **and Hiroshi Ono**[1]

[1]Department of Electrical Engineering, Nagaoka University of Technology, Nagaoka 940-2188, Japan
[2]Department of Creative Technology Engineering, National Institute of Technology, Anan College, Anan 774-0017, Japan
[3]Department of Applied Chemistry, Graduate School of Engineering, University of Hyogo, Himeji 671-2280, Japan

DOI:10.1109/JPHOT.2019.2950021

Manuscript received July 9, 2019; revised September 24, 2019; accepted October 24, 2019. Date of publication October 28, 2019; date of current version November 11, 2019. This work was supported by the JSPS KAKENHI under Grant JP18K04259. Corresponding author: Tomoyuki Sasaki (e-mail: sasaki_tomoy@vos.nagaokaut.ac.jp).

Abstract: We report a terahertz (THz) metamaterial consisting of a metal mesh layer with nematic liquid crystals (LCs). The metal mesh has subwavelength apertures that function as a bandpass filter in the THz spectral range. The LCs are embedded and aligned homogeneously in the apertures. The electromagnetic characteristics were calculated with a finite-difference time-domain method. The metamaterial converts the polarization of the THz wave during transmission and the thickness of the LC layer can be reduced by two orders of magnitude relative to the homogeneously aligned LC without the meta-structures. This increases the response speed to applied external fields. We also fabricated the metamaterial using a dielectric substrate with a metal mesh layer, a nematic LC, and a dielectric substrate with a polymeric alignment layer and investigated its polarization conversion using THz time-domain spectroscopy. The experimental results demonstrated that metal mesh structures with LCs are useful for active THz polarization converters.

Index Terms: Terahertz wave, liquid crystal, metamaterial.

1. Introduction

Active devices that control the propagation of terahertz (THz) waves are in high demand to broaden THz applications [1]–[4]. Electromagnetic metamaterials made from subwavelength unit cells are promising media [5]–[12]. For example, Chen *et al.* proposed a Schottky diode that consisted of an array of metallic meta-atoms on a semiconductor substrate, and demonstrated an electrically tunable THz intensity modulator [5]. Kan *et al.* reported a THz polarization modulator that used a chiral metamaterial with a structure deformable by a pneumatic force [9]. Ling *et al.* proposed a THz metamaterial with a broad negative refractive index band that was thermally tuned via the reversible phase transition of vanadium dioxide [12]. Liquid crystals (LCs) are also promising materials for active optical and THz devices because they exhibit optical anisotropy due to self-assembled molecular alignment, which responds to a variety of external fields [13]–[24]. LCs with a large THz anisotropy of 0.4 have been developed, including useful THz elements with electrical

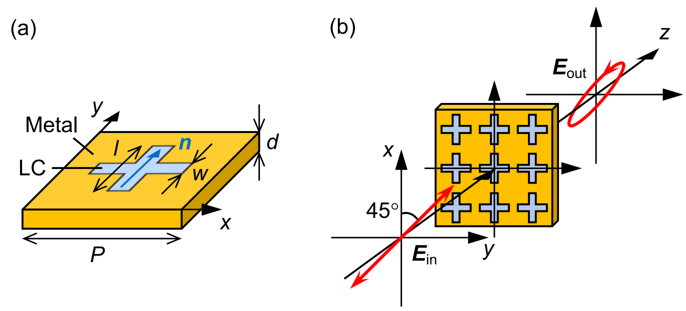

Fig. 1. Schematic illustrations of (a) the unit cell of the LC/metal mesh and (b) the coordinate system for simulating polarization conversion.

tunability [18], [21]. We also reported a THz polarization converter with photothermal control, using a dye-doped LC [23]. However, common LC THz devices have problems with response speed [22], [25]. To obtain sufficient phase shifts or polarization changes for THz waves, the thickness of the LC layer should be comparable to the submillimeter to millimeter wavelength [22]. For example, in homogeneously aligned nematic LCs, the time for the Freedericksz transition for a vertically applied voltage is proportional to the square of the LC layer thickness [26]. Therefore, response times of LC THz devices are much longer than that of LC optical devices [22].

Recently, a new class of THz devices has emerged based on metamaterials with LCs [26]–[36]. Shrekenhamer *et al.* fabricated a tunable absorber by incorporating LCs in strategic locations within the metamaterial unit cell [27]. Buchnev *et al.* demonstrated intensity and phase modulation with a planar metamaterial hybridized with a 12-μm-thick LC layer [28]. Zografopoulos and Beccherelli theoretically postulated that a voltage-controlled metamaterial cavity with a thin nematic LC layer could have millisecond switching times [32]. Thus, LC-loaded metamaterials can be active, functional, compact, and fast THz devices.

Here, we propose a THz polarization converter by combining a subwavelength metal mesh layer with a LC. Metal meshes with subwavelength aperture sizes have been used as bandpass filters [37]–[39]. The LC is embedded and aligned in the apertures to create an anisotropy in the metamaterial that converts the polarization of the transmitted THz wave. The polarization can also be controlled by applying external fields to the LC. We simulated the THz electromagnetic properties of the LC/metal mesh structure using a finite-difference time-domain (FDTD) method, and investigated the relationship between the polarization conversion and the material parameters. We also fabricated the metamaterial to demonstrate the active THz polarization conversion. In the experiment, we used temperature as an external field for simplicity. Our LC-embedded metamaterials realize THz waveplates for a few tens of microns thick, which is substantially thinner than common LC THz waveplates with homogeneous alignment. This is an advantage for the response speed in active control.

2. Theoretical Simulations

Fig. 1(a) shows a schematic of the cross-aperture unit cell of the metal mesh. The arms of the apertures are parallel to the *x*- and *y*-directions and filled with a homogeneously aligned nematic LC. The unit cell size is $P = 0.27$ mm on each side, the arm length is $l = 0.17$ mm, the arm width is w, the thicknesses of the metal layer and the LC layer are both d, the director $\boldsymbol{n}$ (i.e., the optic axis) of the LC is parallel to the *y*-direction. We simulated the power and polarization of a THz wave transmitted at normal incidence through the metal mesh structure via three-dimensional FDTD method. The metal was assumed to be a perfect electric conductor. The incident wave was a linearly polarized THz pulse with an azimuthal angle of 45° [Fig. 1(b)]. In the simulations, the

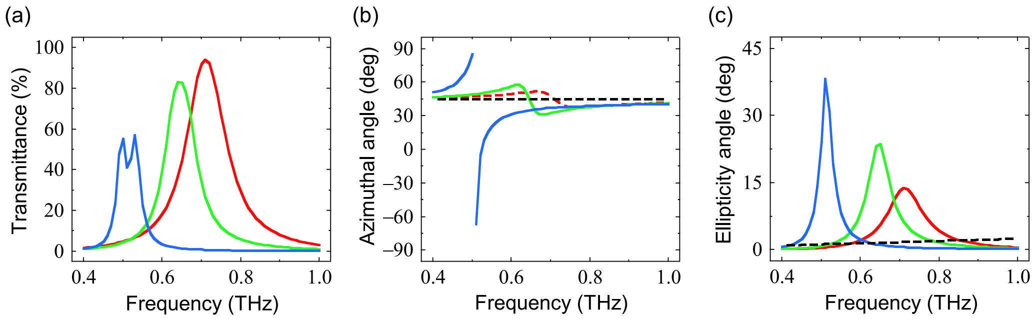

Fig. 2. Simulation results of (a) the transmittance, (b) the azimuthal angle of the transmitted wave, and (c) the ellipticity angle of the transmitted wave for $n_o = 1.54$, $n_e = 1.69$, and $d = 15\ \mu$m. The red, green, and blue lines represent the data for $w = 15\ \mu$m, 30 μm, and 50 μm, respectively. The dashed lines represent simulated results for a homogeneously aligned LC without the meta-structures.

metamaterial was in a vacuum, perfectly matched layers were introduced in the *z*-direction, and periodic boundary conditions were introduced in the *x*- and *y*-directions.

Fig. 2 shows the simulated results for $d = 15\ \mu$m and $w = 15\ \mu$m, 30 μm, and 50 μm. The polarization was represented by the azimuthal angle $\psi = (1/2)\tan^{-1}(S_2/S_1)$ and the ellipticity angle $\chi = (1/2)\tan^{-1}(S_3/\sqrt{S_1^2 + S_2^2})$, where S_1, S_2, and S_3 are the components of the normalized Stokes vector $\boldsymbol{S} = [S_0, S_1, S_2, S_3]^T$ [40]. Here, $-\pi/2 < \psi \leq \pi/2$ and $-\pi/4 \leq \chi \leq \pi/4$, and the linearly polarized incident THz wave has $\psi = \pi/4$ and $\chi = 0$ [40]. The ordinary and extraordinary refractive indices of the LC were set to $n_o = 1.54$ and $n_e = 1.69$, respectively, which are the values of a typical nematic LC 4-penthyl-4'-cyanobiphenyl (5CB) at frequency $f = 1$ THz [41]. The wavelength dispersion and the extinction coefficients were ignored for simplicity. The results indicate that the LC/metal mesh structures convert the polarization of the incident THz wave around the transmission band. The azimuthal and ellipticity angles of the THz wave transmitted through the homogeneously aligned LC layer without metal mesh structures were also calculated for $n_o = 1.54$, $n_e = 1.69$, and $d = 15\ \mu$m, and shown in Figs. 2(b) and 2(c). The data indicate that the LC/metal mesh structures are useful for THz polarization converters. For example, the LC layer thickness should be adjusted to about 1 mm to form a quarter-waveplate (i.e., to convert $\chi = 0$ to $|\chi| = \pi/4$) at $f = 0.5$ THz for a homogeneously aligned LC ($\boldsymbol{n}$ // y) without meta-structures. This was because the retardation must satisfy $|n_e - n_o|d = \lambda/4$, where λ is the wavelength ($\lambda = 0.6$ mm at $f = 0.5$ THz). In contrast, Figs. 2(b) and 2(c) reveal that LC/metal mesh structures form a quarter-waveplate at a subwavelength thickness. This is useful for active control of polarized THz waves. However, Fig. 2 also indicates that LC/metal mesh structures have a trade-off between transmittance and polarization conversion as a function of *w*.

Fig. 3 shows the simulation results for $w = 50\ \mu$m and $d = 15\ \mu$m, 30 μm, and 50 μm. The other parameters are given above. Fig. 4 shows simulation results for $d = 15\ \mu$m, $w = 50\ \mu$m, and $\{n_o, n_e\} = \{1.54, 1.60\}$ or $\{1.55, 1.94\}$. The former set is refractive indices for PCH7, a nematic LC with relatively low THz birefringence [41]. The latter set is refractive indices for LC1825, a nematic LC with relatively high THz birefringence [18], [21]. The other parameters are given above. These results indicate that polarization conversion by the LC/metal mesh structures could be improved with increasing thickness and birefringence. In contrast, the peak value of the transmittance decreased with increasing thickness and birefringence. For practical applications, these material parameters and the aperture pattern should be optimized.

3. Experimental Demonstration

A LC/metal mesh structure was fabricated, as shown schematically in Fig. 5(a). The LC (5CB, Tokyo Chemical Industry, Japan) was located in the apertures using two substrates. The gold

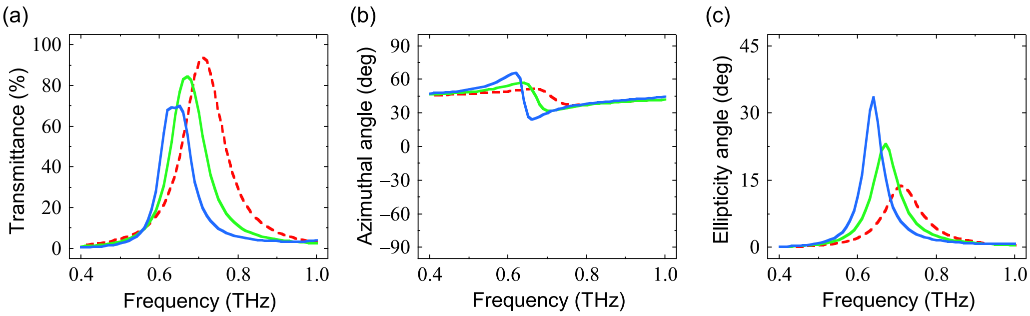

Fig. 3. Simulation results for (a) the transmittance, (b) the azimuthal angle of the transmitted wave, and (c) the ellipticity angle of the transmitted wave for $n_o = 1.54$, $n_e = 1.69$, and $w = 50$ μm. The red, green, and blue lines represent the data for $d = 15$ μm, 30 μm, and 50 μm, respectively (the red lines are the same data shown in Fig. 2).

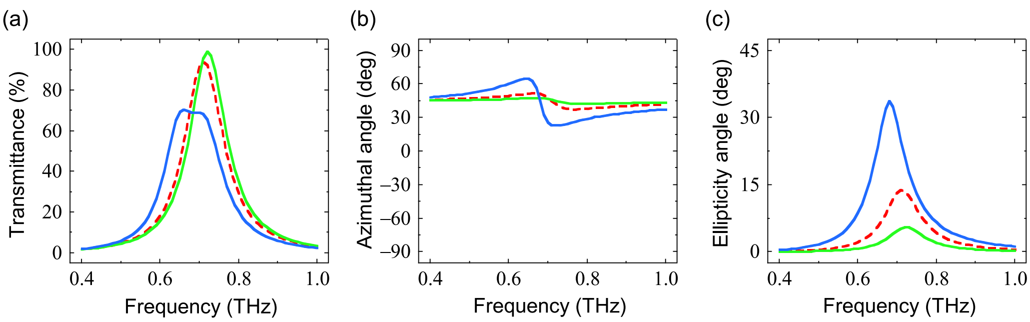

Fig. 4. Simulation results for (a) the transmittance, (b) the azimuthal angle of the transmitted wave, and (c) the ellipticity angle of the transmitted wave for $d = 15$ μm and $w = 50$ μm. The red, green, and blue lines represent the data for $\{n_o, n_e\} = \{1.54, 1.69\}$, $\{1.54, 1.60\}$,and $\{1.55, 1.94\}$, respectively (the red lines are the same data shown in Fig. 2).

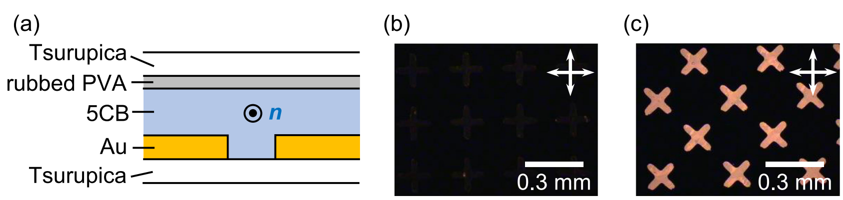

Fig. 5. Fabricated metamaterial. (a) Schematic illustration of the structure in the *xz*-plane, and the polarization optical microscope images, (b) in the dark state, and (c) in the bright state. The arrows represent the transmission axes of the polarizer and analyzer.

mesh was prepared photolithographically with a Galvano scanner. The fabrication process was reported previously [42]. A negative-type photoresist (FNPR-L3, Fuji Chemicals Industrial, Japan) and a 2-mm-thick Tsurupica resin substrate (Pax, Japan), which is highly transparent in the THz spectral range, were used. The mesh dimensions were $P = 270$ μm, $l = 165$ μm, $w = 35$ μm, and $d = 0.2$ μm, as measured with an optical interference microscope (VertScan, Ryoka Systems, Japan). Another substrate coated with a polyvinyl alcohol film and rubbed unidirectionally was used to align the LC [Fig. 5(a)]. The substrates were separated with 20-μm-thick spacers to inject the LC. Polarization optical microscope images in Figs. 5(b) and 5(c) of the LC/metal mesh structure indicate that the LC was uniaxially aligned in the cell. The transmittance and polarization conversion properties were determined with a THz time-domain spectroscopy system (TAS7500, Advantest,

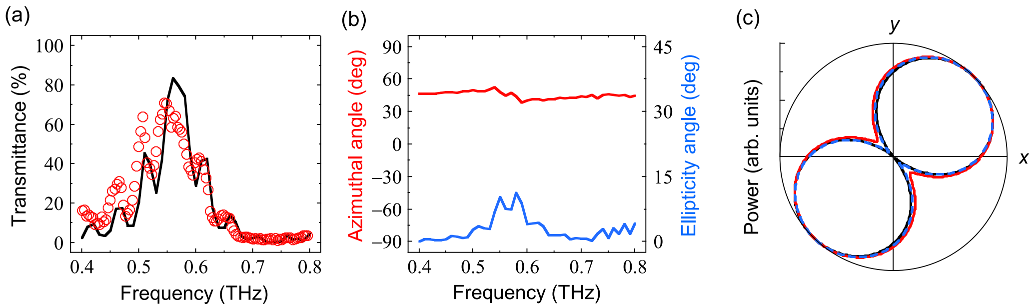

Fig. 6. Properties of the fabricated metamaterial. (a) The transmittance, (b) the azimuthal angle and the ellipticity angle of the transmitted wave, and (c) the polar plots of the transmitted waves. For (a), the circles represent the measured data and the line represents the simulation. For (b), the red line represents the simulated azimuthal angle and the blue line represents the simulated ellipticity angle. For (c), the black line represents the data for $\boldsymbol{E}_{\text{in}}$, the red line represents the data for $\boldsymbol{E}_{\text{out}}$ at the LC temperature, and the blue line represents the data for $\boldsymbol{E}_{\text{out}}$ at the isotropic temperature.

Japan) with photoconductive antennas that emitted and detected linearly polarized THz pulses. The polarization directions of the antennas were arranged 45° to the *x*-axis [Fig. 1(b)].

Fig. 6(a) shows the measured and calculated transmittance, and Fig. 6(b) shows the calculated polarization of the transmitted THz wave. The measurements were conducted at 27°C, which is a LC phase temperature of 5CB. In the calculation, the thickness of the substrate was 2 mm, the refractive index of the substrate was $1.52 + i4\times10^{-4}$, $n_o = 1.55 + i0.025$, and $n_e = 1.69 + i0.01$ [23], [41]. For simplicity, the frequency dispersions of these optical constants were ignored, and the other parameters are given above. The measured transmittance was in rough agreement with the simulation [Fig. 6(a)]. The major cause of the difference between the measured and calculated transmittance is probably the discrepancy between the structure of the fabricated metal mesh layer and the theoretical model. For example, the fabricated cross-apertures are roundish [Fig. 5(c)]. For the metal mesh monolayer with the substrate (without the LC), we observed the same difference between the measurement and the simulation. Fig. 6(c) shows the polar plots of the measured polarization of the incident and transmitted THz waves around $f = 0.55$ THz. These data were acquired by rotating a wire grid polarizer (POL-HDPE-CA25, TYDEX, Russia) in front of the detector. We estimated ψ and $|\chi|$ based on the detected power, and then determined the normalized Jones vectors of the incident and transmitted THz waves ($\boldsymbol{E}_{\text{in}}$ and $\boldsymbol{E}_{\text{out}}$) [42]. The data in Fig. 6(c) show $10\log_{10}|E_x \cos\alpha + E_y \sin\alpha|^2$, where E_x and E_y are the *x*- and *y*-components of $\boldsymbol{E}_{\text{in}}$ or $\boldsymbol{E}_{\text{out}}$, respectively, and $\alpha = \tan^{-1}(y/x)$. Estimated $\{\psi, |\chi|\}$ were $\{45°, 16°\}$ for $\boldsymbol{E}_{\text{in}}$, and $\{46°, 20°\}$ for $\boldsymbol{E}_{\text{out}}$, respectively. The χ of an ideal linearly polarized wave is zero, but χ of $\boldsymbol{E}_{\text{in}}$ was not here. However, we observed a significant change in χ between $\boldsymbol{E}_{\text{in}}$ and $\boldsymbol{E}_{\text{out}}$. In order to demonstrate the active tunability of the polarization conversion property, we also determined the polarization of the transmitted THz wave when the LC/metal mesh structure was heated to 60°C, which is an isotropic phase temperature of 5CB. For this $\boldsymbol{E}_{\text{out}}$, we obtained $\{\psi, |\chi|\} = \{46°, 17°\}$. These data are also shown in Fig. 6(c) in a polar plot. $\boldsymbol{E}_{\text{out}}$ at the isotropic temperature and $\boldsymbol{E}_{\text{in}}$ were nearly identical [Fig. 6(c)]. This is because both the LC and crossed apertures have no anisotropy. These results demonstrated that the LC/metal mesh structure converted the polarization of the THz wave and that the polarization conversion could be controlled with external fields.

4. Conclusions

We investigated the THz polarization conversion properties of monolayered metal mesh metamaterials with LCs. FDTD simulations indicated that THz waveplates can be realized using subwavelength-thick metamaterials, whereas THz waveplates using only LCs need a thickness larger than the wavelength. The LC/metal mesh structure will improve the response speed for external fields. The polarization conversion was confirmed experimentally with a LC/metal mesh structure fabricated with a laser-beam drawing system. The response of the polarization conversion to external fields was demonstrated with a thermal controller. For practical applications, the material parameters and the methods for applying external fields should be optimized in more detail. However, the usefulness of the metamaterials with LCs for THz polarization conversion was demonstrated here.

References

[1] D. Dragoman and M. Dragoman, "Terahertz fields and applications," *Prog. Quantum Electron.*, vol. 28, no. 1, pp. 1–66, 2004.
[2] M. Tonouchi, "Cutting-edge terahertz technology," *Nature Photon.*, vol. 1, no. 2, pp. 97–105, 2007.
[3] J. Federici and L. Moeller, "Review of terahertz and subterahertz wireless communications," *J. Appl. Phys.*, vol. 107, no. 11, 2010, Art. no. 111101.
[4] R. Degl'Innocenti, S. J. Kindness, H. E. Beere, and D. A. Ritchie, "All-integrated terahertz modulators," *Nanophotonics*, vol. 7, no. 1, pp. 127–144, 2018.
[5] H.-T. Chen, W. J. Padilla, J. M. O. Zide, A. C. Gossard, A. J. Taylor, and R. D. Averitt, "Active terahertz metamaterial devices," *Nature*, vol. 444, no. 7119, pp. 597–600, 2006.
[6] J. Gu *et al.*, "Active control of electromagnetically induced transparency analogue in terahertz metamaterials," *Nature Commun.*, vol. 3, 2012, Art. no. 1151.
[7] W. M. Zhu *et al.*, "Microelectromechanical Maltese-cross metamaterial with tunable terahertz anisotropy," *Nature Commun.*, vol. 3, 2012, Art. no. 1274.
[8] D. Wang *et al.*, "Switchable ultrathin quarter-wave plate in terahertz using active phase-change metasurface," *Sci. Rep.*, vol. 5, 2015, Art. no. 15020.
[9] T. Kan *et al.*, "Enantiomeric switching of chiral metamaterial for terahertz polarization modulation employing vertically deformable MEMS spirals," *Nature Commun.*, vol. 6, 2015, Art. no. 8422.
[10] Y. Bai *et al.*, "Optically controllable terahertz modulator based on electromagnetically-induced-transparency-like effect," *Opt. Commun.*, vol. 353, pp. 83–89, 2015.
[11] D.-S. Yang, T. Jiang, and X.-A. Cheng, "Optically controlled terahertz modulator by liquid-exfoliated multilayer WS_2 nanosheets," *Opt. Exp.*, vol. 25, no. 14, pp. 16364–16377, 2017.
[12] F. Ling, Z. Zhong, R. Huang, and B. Zhang, "A broadband tunable terahertz negative refractive index metamaterial," *Sci. Rep.*, vol. 8, no. 1, 2018, Art. no. 9843.
[13] T. Nose, S. Sato, K. Mizuno, J. Bae, and T. Nozokido, "Refractive index of nematic liquid crystals in the submillimeter wave region," *Appl. Opt.*, vol. 36, no. 25, pp. 6383–6387, 1997.
[14] C.-Y. Chen, T.-R. Tsai, C.-L. Pan, and R.-P. Pan, "Room temperature terahertz phase shifter based on magnetically controlled birefringence in liquid crystals," *Appl. Phys. Lett.*, vol. 83, no. 22, pp. 4497–4499, 2003.
[15] H.-Y. Wu, C.-F. Hsieh, T.-T. Tang, R.-P. Pan, and C.-L. Pan, "Electrically tunable room-temperature 2π liquid crystal terahertz phase shifter," *IEEE Photon. Technol. Lett.*, vol. 18, no. 14, pp. 1488–1490, Jul. 2006.
[16] Q. Song *et al.*, "Liquid-crystal-based tunable high-Q directional random laser from a planar random microcavity," *Opt. Lett.*, vol. 32, no. 4, pp. 373–375, 2007.
[17] S. Xiao, Q. Song, F. Wang, L. Liu, J. Liu, and L. Xu, "Switchable random laser from dye-doped polymer dispersed liquid crystal waveguides," *IEEE J. Quantum Electron.*, vol. 43, no. 5, pp. 407–410, May 2007.
[18] M. Reuter *et al.*, "Highly birefringent, low-loss liquid crystals for terahertz applications," *APL Matter.*, vol. 1, no. 1, 2013, Art. no. 012107.
[19] T. Sasaki, K. Noda, N. Kawatsuki, and H. Ono, "Universal polarization terahertz phase controllers using randomly aligned liquid crystal cells with graphene electrodes," *Opt. Lett.*, vol. 40, no. 7, pp. 1544–1547, 2015.
[20] C.-S. Yang, C. Kuo, C.-C. Tang, J. C. Chen, R. P. Pan, and C.-L. Pan, "Liquid-crystal terahertz quarter-wave plate using chemical-vapor-deposited graphene electrodes," *IEEE Photon. J.*, vol. 7, no. 6, Dec. 2015, Art. no. 2200808.
[21] X. Li, N. Tan, M. Pivnenko, J. Sibik, J. A. Zeitler, and D. Chu, "High-birefringence nematic liquid crystal for broadband THz applications," *Liquid Cryst.*, vol. 43, no. 7, pp. 955–962, 2016.
[22] T. Sasaki *et al.*, "Twisted nematic liquid crystal cells with rubbedpoly(3,4-ethylenedioxythiophene)/poly(styrenesulfonate) films for active polarization control of terahertz waves," *J. Appl. Phys.*, vol. 121, no. 14, 2017, Art. no. 143106.
[23] T. Sasaki, H. Okuyama, M. Sakamoto, K. Noda, N. Kawatsuki, and H. Ono, "Optical control of polarized terahertz waves using dye-doped nematic liquid crystals," *AIP Adv.*, vol. 8, no. 11, 2018, Art. no. 115326.
[24] T. Sasaki *et al.*, "Liquid crystal cells with subwavelength metallic gratings for transmissive terahertz elements with electrical tunability," *Opt. Commun.*, vol. 431, pp. 63–67, 2019.
[25] B. Vasić, D. C. Zografopoulos, G. Isić, R. Beccherelli, and R. Gajić, "Electrically tunable terahertz polarization converter based on overcoupled metal-isolator-metal metamaterials infiltrated with liquid crystals," *Nanotechnology*, vol. 28, no. 12, 2017, Art. no. 124002.
[26] P. Yeh and G. Gu, *Optics of Liquid Crystal Displays*. Hoboken, NJ, USA: Wiley, 1997.
[27] D. Shrekenhamer, W.-C. Chen, and W. J. Padilla, "Liquid crystal tunable metamaterial absorber," *Phys. Rev. Lett.*, vol. 110, no. 17, 2013, Art. no. 177403.
[28] O. Buchnev, J. Wallauer, M. Walther, M. Kaczmarek, N. I. Zheludev, and V. A. Fedotov, "Controlling intensity and phase of terahertz radiation with an optically thin liquid crystal-loaded metamaterial," *Appl. Phys. Lett.*, vol. 103, no. 14, 2013, Art. no. 141904.

[29] L. Liu *et al.*, “Temperature control of terahertz metamaterials with liquid crystals,” *IEEE Trans. Terahertz Sci. Technol.*, vol. 3, no. 6, pp. 827−831, Nov. 2013.
[30] G. Isić, B. Vasić, D. C. Zografopoulos, R. Beccherelli, and R. Gajić, “Electrically tunable critically coupled terahertz metamaterial absorber based on nematic liquid crystals,” *Phys. Rev. Appl.*, vol. 3, no. 6, 2015, Art. no. 064007.
[31] R. Kowerdziej, L. Jaroszewicz, M. Olifierczuk, and J. Parka, “Experimental study on terahertz metamaterial embedded in nematic liquid crystal,” *Appl. Phys. Lett.*, vol. 106, no. 9, 2015, Art. no. 092905.
[32] D. C. Zograopoulos and R. Beccherelli, “Tunable terahertz fishnet metamaterials based on thin nematic liquid crystal layers for fast switching,” *Sci. Rep.*, vol. 5, 2015, Art. no. 13137.
[33] N. Chikhi, M. Lisitskiy, G. Papari, V. Tkachenko, and A. Andreone, “A hybrid tunable THz metadevice using a high birefringence liquid crystal,” *Sci. Rep.*, vol. 6, 2016, Art. no. 34536.
[34] L. Yang, F. Fan, M. Chen, X. Zhang, and S.-J. Chang, “Active terahertz metamaterials based on liquid-crystal induced transparency and absorption,” *Opt. Commun.*, vol. 382, pp. 42−48, 2017.
[35] Z. Yin *et al.*, “Fast-tunable terahertz metamaterial absorber based on polymer network liquid crystal,” *Appl. Sci.*, vol. 8, no. 12, 2018, Art. no. 2454.
[36] R. Kowerdziej, M. Olifiierczuk, and J. Parka, “Thermally induced tunability of a terahertz metamaterial by using a specially designed nematic liquid crystal mixture,” *Opt. Exp.*, vol. 26, no. 3, pp. 2443−2452, 2018.
[37] M. E. MacDonald, A. Alexanian, R. A. York, Z. Popović, and E. N. Grossman, “Spectral transmittance of lossy printed resonant-grid terahertz bandpass filters,” *IEEE Trans. Microw. Theory Techn.*, vol. 48, no. 4, pp. 712−718, Apr. 2000.
[38] A. M. Melo *et al.*, “Metal mesh resonant filters for terahertz frequencies,” *Appl. Opt.*, vol. 47, no. 32, pp. 6064−6069, 2008.
[39] A. Ferraro, D. C. Zografopoulos, R. Caputo, and R. Beccherelli, “Broad- and narrow-line terahertz filtering in frequency-selective surfaces patterned on thin low-loss polymer substrates,” *IEEE J. Sel. Topics Quantum Electron.*, vol. 23, no. 4, Jul.–Aug. 2017, Art. no. 8501308.
[40] D. S. Kliger, J. W. Lewis, and C. E. Randall, *Polarized Light in Optics and Spectroscopy*. Boston, MA, USA: Academic, 1990, pp. 103−129.
[41] N. Vieweg, M. K. Shakfa, B. Scherger, M. Mikulics, and M. Koch, “THz properties of nematic liquid crystals,” *J. Infrared Millimeter Terahertz Waves*, vol. 31, no. 11, pp. 1312−1320, 2010.
[42] T. Sasaki *et al.*, “Effects of slant angle of metallic fish-scale structure on polarization conversion in the terahertz spectral range,” *Appl. Phys. A*, vol. 124, no. 11, 2018, Art. no. 789.